Structural Determinants of the Substrate and Stereochemical Specificity of Phosphotriesterase†

Misty Chen-Goodspeed, Miguel A. Sogorb, Feiyue Wu, Suk-Bong Hong, and Frank M. Raushel*

Department of Chemistry, Texas A&M University, P.O. Box 30012, College Station, Texas 77842-3012

Received July 5, 2000; Revised Manuscript Received October 11, 2000

ABSTRACT: Bacterial phosphotriesterase (PTE) catalyzes the hydrolysis of a wide variety of organophosphate nerve agents and insecticides. Previous kinetic studies with a series of enantiomeric organophosphate triesters have shown that the wild type PTE generally prefers the S_P-enantiomer over the corresponding R_P-enantiomers by factors ranging from 1 to 90. The three-dimensional crystal structure of PTE with a bound substrate analogue has led to the identification of three hydrophobic binding pockets. To delineate the factors that govern the reactivity and stereoselectivity of PTE, the dimensions of these three subsites have been systematically altered by site-directed mutagenesis of Cys-59, Gly-60, Ser-61, Ile-106, Trp-131, Phe-132, His-254, His-257, Leu-271, Leu-303, Phe-306, Ser-308, Tyr-309, and Met-317. These studies have shown that substitution of Gly-60 with an alanine within the *small* subsite dramatically decreased k_{cat} and k_{cat}/K_a for the R_P-enantiomers, but had little influence on the kinetic constants for the S_P-enantiomers of the chiral substrates. As a result, the chiral preference for the S_P-enantiomers was greatly enhanced. For example, the value of k_{cat}/K_a with the mutant G60A for the S_P-enantiomer of methyl phenyl *p*-nitrophenyl phosphate was 13000-fold greater than that for the corresponding R_P-enantiomer. The mutation of I106, F132, or S308 to an alanine residue, which enlarges the *small* or *leaving group* subsites, caused a significant reduction in the enantiomeric preference for the S_P-enantiomers, due to selective increases in the reaction rates for the R_P-enantiomers. Enlargement of the *large* subsite by the construction of an H254A, H257A, L271A, or M317A mutant had a relatively small effect on k_{cat}/K_a for either the R_P- or S_P-enantiomers and thus had little effect on the overall stereoselectivity. These studies demonstrate that by modifying specific residues located within the active site of PTE, it is possible to dramatically alter the stereoselectivity and overall reactivity of the native enzyme toward chiral substrates.

The bacterial phosphotriesterase (PTE)[1] from *Pseudomonas diminuta* has been found to catalyze the hydrolysis of a wide range of organophosphate triesters, including many agricultural insecticides and potent acetylcholinesterase inhibitors (*1*−*3*). To date, the best substrate for this enzyme is paraoxon, which is hydrolyzed at a rate approaching the diffusion-controlled limit ($k_{cat}/K_a \geq 4 \times 10^7$ M^{-1} s^{-1}) (*4*). Shown in Scheme 1 is the enzymatic reaction for the hydrolysis of paraoxon to *p*-nitrophenol and diethyl phosphate. The active site of this enzyme has been shown to contain a binuclear zinc center that is bridged by a carboxylated lysine residue and a hydroxide from the solvent (*5*). The utilization of a chiral organophosphate substrate has demonstrated that the overall reaction proceeds with an inversion of stereochemical configuration at the phosphorus center (*6*). Therefore, the enzymatic reaction is initiated by the direct nucleophilic attack of the hydrolytic water molecule on the phosphorus center without the formation of a phosphorylated enzyme intermediate.

Scheme 1

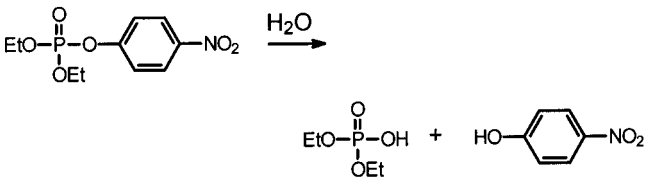

The three-dimensional structure of Zn/Zn-PTE with a bound substrate analogue, diethyl 4-methylbenzylphosphonate, has led to the identification of the locations of three distinct binding pockets that are likely responsible for the orientation of substrates within the active site of this enzyme (*7*). These binding pockets have now been designated as the *small*, *large*, and *leaving group* subsites. The *small* subsite is predominantly defined by the side chains of Gly-60, Ile-106, Leu-303, and Ser-308. Cys-59 and Ser-61 are near this binding pocket, but their side chains are oriented away from this subsite. The pocket for the *large* subsite is largely formed by the side chains originating from His-254, His-257, Leu-271, and Met-317. The residues that are primarily located around the *leaving group* subsite are Trp-131, Phe-132, Phe-306, and Tyr-309. The specific orientation of the bound inhibitor within the active site of PTE is graphically illustrated in Figure 1.

† This work was supported in part by the National Institutes of Health (Grant GM-33894), the Robert A. Welch Foundation (Grant A-840), and the Office of Naval Research (Grant N00014-99-0235). M.A.S. held a fellowship from the Spanish Ministry of Science.

* To whom correspondence should be addressed. Phone: (979) 845-3373. Fax: (979) 845-9452. E-mail: raushel@tamu.edu.

[1] Abbreviation: PTE, phosphotriesterase.

10.1021/bi001548l CCC: $20.00
Published on Web 01/11/2001

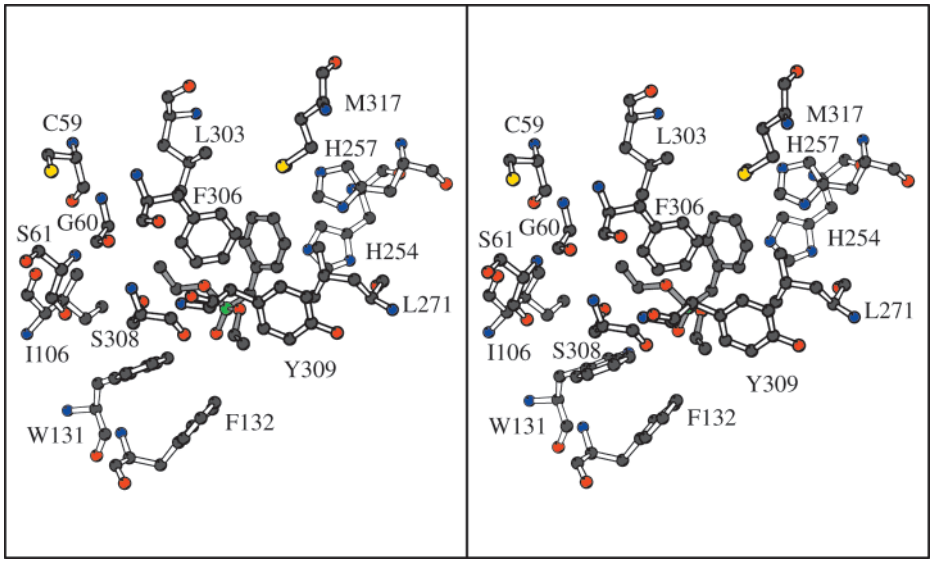

FIGURE 1: Graphic representation of the binding pockets of phosphotriesterase with the bound substrate analogue. The bound substrate analogue is shown in gray. The *small* subsite consists primarily of Gly-60, Ile-106, Leu-303, and Ser-308. The *large* subsite consists mainly of His-254, His-257, Leu-271, and Met-317, while the *leaving group* subsite is surrounded by Trp-131, Phe-132, Phe-306, and Tyr-309. The coordinates are taken from the structure determined by Vanhooke (*7*).

Chart 1

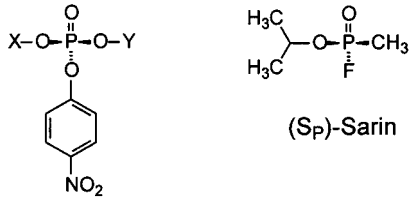

Previous investigations with a variety of organophosphate analogues have demonstrated that the substrate specificity of PTE is reasonably promiscuous (*8*). Recently, a series of achiral and chiral organophosphates, possessing *p*-nitrophenol as the leaving group in combination with either methyl, ethyl, isopropyl, or phenyl as the two nonleaving group substituents, was characterized with PTE (*9*). Within this modest substrate library, the turnover numbers ranged from 220 to 18 200 s^{-1} for Co/Co-PTE. Moreover, for the six possible pairs of chiral organophosphate triesters in this series, the S_P-isomer was invariably preferred over the R_P-isomer by up to 2 orders of magnitude. For example, the value of k_{cat} for the S_P-enantiomer of isopropyl methyl *p*-nitrophenyl phosphate was ~15-fold greater than that for the corresponding R_P-enantiomer (*9*). If the three-dimensional structures of these stereoisomers are modeled into the active site of PTE, using the X-ray structure of the bound inhibitor complex as a guide, then the substituent depicted with a Y in Chart 1 would be bound to the *large* subsite while the substituent depicted with an X would occupy the *small* subsite. For the preferred S_P-stereoisomer in this series of substrates, the substituent represented by Y is physically larger than the substituent represented by X.

The organophosphorus nerve agents, sarin, soman, and VX, all have a chiral phosphorus center. Inhibition studies with acetylcholinesterase have shown that the rate of inactivation by the S_P-enantiomer (see Chart 1) of sarin is 4200 times faster than the rate of inactivation by the R_P-enantiomer (*10*). Thus, the biological toxicity of organophosphates is very much dependent on the absolute configuration at the phosphorus center. The optimization of PTE for the catalytic degradation of toxic chemical nerve agents can only be achieved by increasing the overall rate of hydrolysis for all of the toxic stereoisomers. Therefore, the factors that dictate the stereoselectivity of this enzyme must be identified and more fully understood. In the crystal structure of PTE, there are very few electrostatic interactions between the bound inhibitor and the enzyme (*7*). Thus, the physical size of the binding subsites and hydrophobic interactions must play the dominant roles in determining the substrate selectivity and stereoselectivity of the wild type PTE. In this study, the structural determinants of the chiral selectivity of the wild type PTE have been probed by systematically altering the cavity size of the individual binding pockets through site-directed mutagenesis. The residues that define these subsites were sequentially replaced with alanine in an attempt to elucidate the steric constraints within the active site of PTE. This library of PTE mutants has been characterized with a modest library of 16 organophosphate triesters. These substituents differ widely in their capacity for steric and hydrophobic interactions with the side chains of the active site residues. These studies have demonstrated that the stereoselectivity and overall reactivity of PTE toward chiral and achiral substrates can be dramatically altered and systematically manipulated by a single mutation within the active site of PTE.

MATERIALS AND METHODS

Materials. Paraoxon (*O*,*O*-diethyl-*O*-*p*-nitrophenyl phosphate) was purchased from Sigma Chemical Co. and purified according to a previously described protocol (*11*). All of the other paraoxon analogues (**I**−**X**) were synthesized using variations of published procedures (*9*, *12*, *13*).[2] Restriction enzymes and T4 DNA ligase were acquired from New England Biolabs. Wizard Miniprep DNA purification kits

[2] The toxicity for some of these compounds has not been assessed, and thus, these compounds should be used with caution.

and Magic PCR Prep DNA purification kits were purchased from Promega. GeneClean DNA purification kits were obtained from Bio 101. DNA sequencing reactions and the synthesis of oligonucleotides were carried out by the Gene Technology Laboratory of Texas A&M University. All other chemicals and reagents were purchased from Sigma, United States Biochemical, or Aldrich.

Bacterial Strains and Plasmids. Two strains of *Escherichia coli*, BL-21 (*14*) and XL1-Blue (*15*), were used in this investigation. The pBS$^+$ plasmid (Stratagene) was used in the construction of pJK01 (*16*) and pJW01.[3] These two plasmids contain the *opd* gene that encodes the mature phosphotriesterase without the 29-amino acid leader sequence. Either pJK01 or pJW01 was utilized as the starting template for all mutagenesis experiments.

Site-Directed Mutagenesis. The genes for the M317A and W131A mutants were generated by site-directed mutagenesis with the plasmid pJK01 using the method of overlap extension polymerase chain reaction (PCR) as described previously (*17*). The purified mutagenic PCR fragments were digested with *Bam*HI and ligated with *Bam*HI-digested pBS$^+$ using T4 DNA ligase. Each of the mutated genes was completely sequenced to ensure that only the desired base changes introduced at residue positions 131 and 317 were present. The plasmid pJW01 was used as the template for the construction of C59A, G60A, S61A, I106A, F132A, H254A, H257A, L271A, L303A, F306A, S308A, and Y309A. Unique restriction sites were selected on each side of the codon of the specific amino acid to be mutated. The digested pJW01 fragment was purified by agarose gel electrophoresis and concentrated using the GeneClean system. Each pair of overlapping mutagenic oligonucleotides was annealed for 5 min at 72 °C in the presence of 2 μL of T4 DNA ligase buffer, and then incubated for 1 h at 25 °C. The annealed oligonucleotides were ligated into the pJW01 plasmid using T4 DNA ligase and then transformed into either XL1-Blue or BL-21. The ligated portion of the phosphotriesterase gene was completely sequenced to ensure that only the fragment containing the desired base changes was utilized.

Purification of Wild Type and Mutant Enzymes. The wild type and mutant proteins were purified from BL-21 cells according to the previously reported protocol (*11*). SDS−polyacrylamide gel electrophoresis indicated that all of the mutants were of the same size as the wild type protein and the purity of the proteins was greater than 95%. The apoenzyme was prepared and reconstituted with Co^{2+} according to established procedures (*18*).

Kinetic Characterization. The catalytic activity for the Co/Co-reconstituted mutants of PTE with the library of organophosphate triesters was measured by monitoring the appearance of *p*-nitrophenol at 400 nm (ϵ = 17 000 M^{-1} cm^{-1}) at pH 9.0 and 25 °C using a Gilford model 260 spectrophotometer (*11*). Because of the limited solubility of some compounds, a 20% methanol/water mixture was used in the kinetic analysis of diphenyl *p*-nitrophenyl phosphate (**X**), and a 5% mixture was used for methyl phenyl *p*-nitrophenyl phosphate (**IV**), ethyl phenyl *p*-nitrophenyl phosphate (**VII**), and isopropyl phenyl *p*-nitrophenyl phosphate (**IX**).

[3] Unpublished work of J. Wohlschlegel, Texas A&M University.

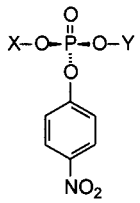

Substrate	X	Y
I	CH_3	CH_3
R_p-II	CH_2CH_3	CH_3
S_p-II	CH_3	CH_2CH_3
R_p-III	$CH(CH_3)_2$	CH_3
S_p-III	CH_3	$CH(CH_3)_2$
R_p-IV	C_6H_5	CH_3
S_p-IV	CH_3	C_6H_5
V	CH_2CH_3	CH_2CH_3
R_p-VI	$CH(CH_3)_2$	CH_2CH_3
S_p-VI	CH_2CH_3	$CH(CH_3)_2$
R_p-VII	C_6H_5	CH_2CH_3
S_p-VII	CH_2CH_3	C_6H_5
VIII	$CH(CH_3)_2$	$CH(CH_3)_2$
R_p-IX	C_6H_5	$CH(CH_3)_2$
S_p-IX	$CH(CH_3)_2$	C_6H_5
X	C_6H_5	C_6H_5

FIGURE 2: Structures of the organophosphates used in the substrate library for this investigation.

Data Analysis. The kinetic parameters (V_m and K_a) were determined by fitting the experimental data to eq 1, using a computer program provided by Savanna Shell Software.

$$v = V_m A/(K_a + A) \quad (1)$$

where v is the initial velocity, V_m is the maximum velocity, K_a is the Michaelis constant, and A is the substrate concentration.

RESULTS

Preparation of Protein and Substrate Libraries. Fourteen amino acids within the active site of PTE were sequentially substituted with alanine in an attempt to identify the roles of individual side chains in defining the substrate reactivity and stereoselectivity of this enzyme. The particular residues were selected for mutation on the basis of the X-ray crystal structure of PTE containing a bound substrate analogue (*7*). All of the mutant enzymes were expressed and purified to homogeneity as judged by SDS−polyacrylamide gel electrophoresis. The properties of the wild type and mutant forms of PTE were characterized with a series of organophosphate triesters containing *p*-nitrophenol as the leaving group. The structures of the organophosphates within the substrate library are presented in Figure 2. The kinetic constants for the

Table 1: Maximum Velocity (s^{-1}) for the Hydrolysis of Achiral and Chiral Phosphotriesters by Co/Co-PTE[a]

substrate	WT	C59A	G60A	S61A	I106A	W131A	F132A	H254A	H257A	L271A	L303A	F306A	S308A	Y309A	M317A
I	1.8e4	8.4e3	1.5e4	3.2e4	6.6e3	1.1e3	5.5e3	4.6e3	4.9e3	1.6e3	3.3e3	6.5e0	1.7e4	4.9e2	1.8e3
(R_P)-**II**	1.4e4	4.9e3	4.3e3	8.9e3	1.2e4	1.7e3	1.8e4	1.6e3	2.1e3	4.0e3	7.6e3	1.1e2	1.7e4	3.6e3	6.2e3
(S_P)-**II**	1.5e4	6.3e3	2.1e4	2.1e4	1.2e4	3.1e3	1.8e4	1.2e3	2.7e3	3.9e3	4.6e3	1.1e2	9.8e3	8.4e3	5.3e3
(R_P)-**III**	5.0e2	4.3e2	6.7e1	8.2e2	1.5e3	3.7e1	1.7e3	1.7e2	3.1e2	1.9e3	1.1e3	4.9e0	1.4e3	3.9e2	1.8e3
(S_P)-**III**	7.1e3	3.3e3	9.8e3	7.5e3	5.8e3	1.6e3	8.9e3	1.0e3	1.5e3	2.1e3	7.2e3	2.6e2	1.5e4	4.3e3	5.9e3
(R_P)-**IV**	3.7e2	1.0e2	1.9e1	6.0e2	5.0e3	7.4e2	1.4e4	2.2e2	2.9e1	2.2e2	4.7e2	2.6e1	2.1e3	4.1e2	3.6e1
(S_P)-**IV**	4.1e4	8.5e3	4.2e4	1.4e4	2.3e4	4.3e3	1.9e4	5.3e3	2.3e3	5.7e3	6.3e3	4.8e3	2.4e4	4.4e3	4.6e3
V	7.1e3	4.9e3	8.7e3	7.4e3	1.2e4	5.3e3	8.4e3	1.8e3	1.4e3	4.1e3	6.3e3	7.4e2	6.9e3	8.1e3	4.7e3
(R_P)-**VI**	7.1e2	1.8e2	1.3e3	3.1e2	2.3e3	2.6e2	7.0e2	1.5e2	2.2e2	2.6e1	3.3e2	8.4e0	4.5e2	2.2e2	1.2e2
(S_P)-**VI**	3.0e3	2.0e3	4.7e3	2.0e3	4.2e3	1.2e3	2.6e3	2.1e3	1.8e3	3.1e3	3.8e3	8.5e2	3.7e3	5.0e3	2.0e3
(R_P)-**VII**	1.0e3	5.6e2	4.9e0	8.1e2	3.9e3	9.1e2	4.6e3	2.0e2	1.1e2	8.6e2	8.2e2	9.7e2	4.1e3	7.4e2	5.8e1
(S_P)-**VII**	9.5e3	3.3e3	4.6e3	4.1e3	1.1e4	5.1e3	1.0e4	1.9e3	9.3e2	2.3e4	1.8e4	1.9e3	1.4e4	2.8e3	3.4e3
VIII	2.2e2	1.0e2	1.0e2	2.2e2	5.4e2	2.0e1	2.2e2	5.7e1	4.5e1	3.3e1	1.8e1	4.0e0	2.2e2	3.7e2	1.2e2
(R_P)-**IX**	5.3e2	2.4e2	0.3e0	1.1e3	3.1e3	2.6e2	4.3e3	2.0e2	1.4e1	2.3e1	2.8e1	0.9e0	1.4e3	7.2e1	9.5e0
(S_P)-**IX**	2.6e3	8.9e2	3.9e3	9.6e2	3.9e3	1.0e3	1.7e3	5.6e2	6.2e2	7.4e2	1.2e3	6.2e2	6.9e3	2.3e3	8.3e2
X	3.4e3	9.7e2	1.0e1	2.8e3	2.2e3	4.5e2	7.4e2	5.6e2	1.0e3	4.6e2	2.5e2	4.1e1	2.2e3	1.7e2	4.1e2

[a] The values were obtained by a fit of the data at pH 9.0 and 25 °C to eq 1. The standard error in every case was less than 20% of the stated values.

Table 2: Values of k_{cat}/K_a (M^{-1} s^{-1}) for the Hydrolysis of Achiral and Chiral Phosphotriesters by Co/Co-PTE[a]

substrate	WT	C59A	G60A	S61A	I106A	W131A	F132A	H254A	H257A	L271A	L303A	F306A	S308A	Y309A	M317A
I	1.2e7	4.5e6	1.0e7	6.0e6	3.6e6	1.9e5	6.7e6	6.9e6	1.7e6	4.6e5	9.0e5	9.2e3	1.6e7	2.5e5	1.5e6
(R_P)-**II**	3.2e7	1.3e7	8.7e6	2.1e7	1.7e7	9.7e5	3.3e7	2.8e7	4.9e6	3.1e6	4.0e6	5.6e4	2.4e7	1.2e6	4.3e6
(S_P)-**II**	3.4e7	1.4e7	9.9e7	2.0e7	2.4e7	2.0e6	4.4e7	2.2e7	3.6e6	3.0e6	3.8e6	5.7e4	1.9e7	2.2e6	7.5e6
(R_P)-**III**	8.5e5	1.1e6	1.2e5	8.9e5	1.5e6	3.0e4	1.4e6	6.3e5	1.8e5	4.6e5	3.0e5	3.1e3	6.4e5	1.4e5	3.1e5
(S_P)-**III**	2.7e7	1.7e7	4.8e7	9.8e6	1.3e7	1.2e6	1.6e7	1.6e7	4.1e6	3.0e6	7.6e6	1.3e5	3.8e7	1.8e6	2.9e6
(R_P)-**IV**	1.0e6	3.3e5	1.7e4	1.4e6	2.5e7	2.9e6	1.3e7	1.1e6	1.4e5	6.4e5	9.1e5	3.2e4	3.6e6	8.7e5	2.0e5
(S_P)-**IV**	9.3e7	3.6e7	2.2e8	5.9e7	7.2e7	1.4e7	6.1e7	5.3e7	1.2e7	2.9e7	2.3e7	5.1e6	5.1e7	8.7e6	2.4e7
V	6.4e7	2.7e7	4.2e7	4.7e7	3.8e7	8.3e6	3.4e7	3.1e7	3.4e6	1.2e7	9.0e6	2.3e5	4.0e7	6.1e6	1.9e7
(R_P)-**VI**	4.1e6	1.9e6	2.7e6	4.2e6	9.1e6	3.6e5	2.3e6	3.3e5	2.2e5	3.9e5	1.8e5	2.2e4	6.5e5	4.7e5	5.3e5
(S_P)-**VI**	4.2e7	2.5e7	6.5e7	2.6e7	2.7e7	7.5e6	1.5e7	9.5e6	3.3e6	6.8e6	3.0e6	3.0e5	7.0e6	6.1e6	6.6e6
(R_P)-**VII**	3.7e6	4.1e6	1.6e4	8.8e6	2.8e7	1.3e6	1.8e7	5.5e6	1.0e6	6.6e6	2.4e6	7.2e5	3.4e7	1.2e6	3.0e6
(S_P)-**VII**	7.6e7	8.6e7	1.8e8	9.4e7	4.7e7	1.8e7	5.0e7	2.4e7	1.7e7	7.4e7	4.3e7	1.3e7	1.6e8	9.8e6	1.7e7
VIII	4.8e6	1.0e6	1.9e5	2.9e6	6.9e6	8.6e4	1.9e6	1.1e6	4.8e5	1.5e5	1.3e5	1.7e4	3.7e6	2.4e5	4.8e5
(R_P)-**IX**	5.2e6	3.0e5	6.2e3	3.3e6	2.1e7	1.0e6	2.3e7	5.5e6	2.1e5	2.5e5	1.4e5	1.5e4	1.7e6	2.3e5	4.3e5
(S_P)-**IX**	1.8e8	2.8e7	9.2e7	4.4e7	5.2e7	1.0e7	1.2e8	3.6e7	7.7e6	6.7e6	3.8e6	1.5e6	2.3e7	8.1e6	1.0e7
X	1.6e7	6.0e6	9.6e4	1.2e7	1.3e7	8.4e6	2.1e7	4.7e6	9.2e6	4.7e6	7.7e6	4.8e5	7.9e7	7.6e6	5.3e6

[a] The values were obtained by a fit of the data at pH 9.0 and 25 °C to eq 1. The standard error in every case was less than 20% of the stated values.

hydrolysis of the 16 achiral and chiral organophosphate triesters are summarized in Tables 1 and 2. The stereoselectivity of each mutant toward the six pairs of chiral enantiomers is reported as the ratio of k_{cat}/K_a for the S_P-enantiomer relative to that for the R_P-enantiomer, and the results are presented in Table 3.

Modifications to the Small Subsite. The substitution of the *small* subsite residue, Gly-60, with an alanine decreased the size of the cavity for this binding pocket. G60A exhibited a 340-fold decrease in k_{cat} for diphenyl *p*-nitrophenyl phosphate (**X**) but an only 2-fold reduction in k_{cat} for diisopropyl *p*-nitrophenyl phosphate (**VIII**) relative to that of the wild type enzyme. The k_{cat}/K_a values of G60A for **VIII** and **X** were reduced by factors of 25 and 167, respectively. The kinetic constants of G60A with dimethyl *p*-nitrophenyl phosphate (**I**) and diethyl *p*-nitrophenyl phosphate (**V**) were essentially identical to those of the native enzyme. With the wild type enzyme, all of the S_P-enantiomers of the chiral organophosphate triesters are better substrates than the corresponding R_P-enantiomers. This stereoselective preference for the S_P-enantiomers increases significantly when Gly-60 is replaced with an alanine. The G60A mutant showed reductions in k_{cat} of up to 1800-fold for the R_P-enantiomers relative to that of the wild type enzyme. The most severe losses in the catalytic activity of G60A were observed for the hydrolysis of the R_P-enantiomers containing a single phenyl substituent (**IV**, **VII**, and **IX**), whereas smaller reduction factors were observed for the hydrolysis of the R_P-enantiomers containing only alkyl substituents (**II**, **III**, and

Table 3: k_{cat}/K_a Ratios for the Hydrolysis of Chiral Substrates by Co/Co-PTE[a]

mutant	**II**	**III**	**IV**	**VI**	**VII**	**IX**
WT	1	32	90	10	21	35
C59A	1	15	110	13	21	93
G60A	12	410	13000	24	11000	15000
S61A	1	11	43	6	11	13
I106A	1	9	3	3	2	3
W131A	2	40	5	21	14	10
F132A	1	12	5	6	3	5
H254A	1	25	48	29	4	7
H257A	1	23	86	15	17	37
L271A	1	7	45	17	11	27
L303A	1	25	25	17	18	27
F306A	1	42	160	14	18	100
S308A	1	59	14	11	5	14
Y309A	2	13	10	13	8	35
M317A	2	9	120	13	6	24

[a] This ratio was determined according to the equation $S_P/R_P = (k_{cat}/K_a)_S/(k_{cat}/K_a)_R$.

VI). However, the G60A mutant displayed kinetic constants for all of the S_P-enantiomers that were essentially the same as that of the wild type enzyme. Therefore, the catalytic preferences exhibited for the S_P-enantiomers within the substrate library by the mutant G60A are significantly greater than that possessed by the wild type enzyme.

The *small* subsite was slightly enlarged by the substitution of Ile-106 with an alanine residue. This modification to the active site gives rise to significant enhancements in the catalytic constants for the R_P-enantiomers relative to that of the wild type enzyme. Most notably, the k_{cat} and k_{cat}/K_a values for the R_P-enantiomers containing a single phenyl substituent (**IV**, **VII**, and **IX**) were increased more than those for the other substrates without a phenyl substituent (**II**, **III**, and **VI**). However, introduction of an alanine at position 106 also caused small reductions in k_{cat} and k_{cat}/K_a for the S_P-enantiomers. Consequently, there was a significant drop in the catalytic preferences for the S_P-enantiomers over the corresponding R_P-enantiomers with this mutant for substrates **IV**, **VI**, **VII**, and **IX**. This relaxation in the stereoselectivity of PTE was accomplished while maintaining most of the catalytic power for the initially faster S_P-isomers.

Mutation of Ser-308 to an alanine also enlarged the size of the *small* subsite. The catalytic constants displayed by S308A for the R_P-enantiomers of **IV**, **VII**, and **IX** were increased up to 9-fold, whereas the catalytic constants for the S_P-enantiomers were relatively unaffected by this mutation. Therefore, the stereoselectivity for the S_P-enantiomers of **IV**, **VII**, and **IX** was reduced with this mutation. For chiral substrates **II**, **III**, and **VI**, this mutant had a minimal effect on either the magnitude of the kinetic constants or the stereoselectivity. Leu-303 is also located in the *small* subsite; however, mutation of this residue to an alanine did not result in any systematic alterations in the catalytic constants for the substrate library, and thus, the overall stereoselectivity is nearly the same as that found with the wild type enzyme. Mutants C59A and S61A had kinetic properties for most of the substrates that were essentially identical with those of the wild type enzyme.

Modifications to the Large Subsite. The mutations that are localized predominantly within the *large* subsite, H254A, H257A, L271A, and M317A, displayed catalytic activities that were very similar to one another. In general, the values for k_{cat} and k_{cat}/K_a obtained for these mutants with the organophosphate substrate library were reduced relative to those of the wild type enzyme. Reductions in the rate constants were limited to about 1 order of magnitude, with H254A showing the greatest overall losses. However, there were no significant changes to the chiral selectivity exhibited by these mutants relative to that of the wild type enzyme. In every case, these mutants preferred the S_P-enantiomers over the R_P-enantiomers by about the same factor as the wild type enzyme. The diminution of the catalytic rate constants is thus most likely to be due to global, rather than local, effects on the enzyme active site. These results also indicate that the *large* subsite within the wild type enzyme can adequately accommodate the substituents utilized for the substrate library created for this investigation. With these substituents, nothing is gained from an expansion of the large subsite.

Modifications to the Leaving Group Subsite. The four aromatic residues mutated for this investigation are all positioned near the *leaving group* subsite. The F132A mutant exhibited 5−38-fold increases in k_{cat} for the R_P-enantiomers of **IV**, **VII**, and **IX**, but displayed approximately the same values of k_{cat} for the S_P-enantiomers as the wild type enzyme. The k_{cat}/K_a values for the R_P-enantiomers of **IV**, **VII**, and **IX** were increased 4−13-fold, whereas the k_{cat}/K_a values for the corresponding S_P-enantiomers were slightly reduced relative to that of the wild type enzyme. Thus, substitution of Phe-132 with an alanine virtually eliminated the stereoselectivity for the enantiomers of **IV**, **VII**, and **IX** observed with the native enzyme. The tryptophan at position 131 is located between the *small* and *leaving group* subsites. For chiral substrates **IV**, **VII**, and **IX**, the k_{cat} and k_{cat}/K_a values of W131A for the S_P-enantiomers were reduced whereas the kinetic constants for the R_P-enantiomers were virtually the same as those of the wild type enzyme. Hence, the stereoselectivity for the S_P-enantiomers of **IV**, **VII**, and **IX** was reduced upon replacing Trp-131 with an alanine. For the remaining substrates, W131A displayed reductions in catalytic activity of up to 18-fold when compared with the wild type enzyme. This mutant had little effect on the overall enantiomeric selectivity for chiral substrates **II**, **III**, and **VI**. Tyr-309 is also located within the *leaving group* subsite. Y309A displayed reductions in the catalytic constants by factors up to 36-fold relative to those of the wild type enzyme. For all of the substrates (**I**−**X**), the k_{cat}/K_a values of Y309A were lower than that of the native enzyme by up to 27-fold. Phe-306 is positioned at the interface of the three binding subsites. The maximal rates of hydrolysis for all substrates were suppressed with F306A when compared with that of the wild type enzyme. The F306A mutation resulted in reductions in the kinetic constants by 1−3 orders of magnitude for most of the substrates tested, and thus, a significant fraction of the inherent catalytic activity of PTE has been lost with this alteration to the active site.

DISCUSSION

The bacterial phosphotriesterase has been shown to hydrolyze the S_P-enantiomers of organophosphate triesters at significantly faster rates than the corresponding R_P-enantiomers (*9*). The determination of the three-dimensional structure of PTE with a bound substrate analogue has provided the essential structural information for the identification of the potential ligand interactions within the enzyme−inhibitor complex. Modeling of the preferred enantiomer of organophosphate triesters into the active site of PTE has outlined three distinct regions (*small*, *large*, and *leaving group*) that are potentially involved in the binding of the substituents attached to the tetrahedral phosphorus center of good substrates. The observed substrate selectivity exhibited by the wild type PTE must reflect the stereochemical constraints within each of these subsites. The crystal structure of PTE shows that the subsites for the binding of substrates to the active site of PTE consist primarily of hydrophobic residues. Thus, site-directed mutagenesis was employed to systematically alter the three binding regions by replacing the residues that define these subsites with the sterically conservative amino acid, alanine. By taking advantage of the broad substrate specificity of PTE, we tested a series of organophosphate triesters with different substituents attached to the phosphate center with these mutant enzymes. These mutations, directed at the steric and hydrophobic interactions between the inhibitor and the side chains

of the active site residues, serve as reporters of the stereochemical determinants that govern the substrate reactivity and stereoselectivity of wild type PTE.

The crystal structure of PTE indicates that Gly-60 is positioned in the *small* subsite (*7*). Mutation of Gly-60 to an alanine resulted in a mutant enzyme with wild type activity when tested with dimethyl and diethyl *p*-nitrophenyl phosphate. However, the catalytic activity with diphenyl *p*-nitrophenyl phosphate was reduced by 2 orders of magnitude. It thus appears that reducing the cavity size of the *small* subsite by adding a single methyl group significantly increases the steric constraints for substrates that require a large substituent to be bound to this region of the active site. G60A displayed wild type levels of activity for the hydrolysis of the S_P-enantiomers of the organophosphate triester library. Moreover, the catalytic activities of G60A for the hydrolysis of the R_P-enantiomers containing a single phenyl substituent were substantially reduced, which is consistent with the proposed spatial orientation of this enantiomer within the active site of PTE. Therefore, the overall stereoselectivity of G60A for the faster S_P-enantiomers was increased by up to 3 orders of magnitude relative to that for the slower R_P-enantiomers (Table 3). The catalytic rates of G60A toward the R_P-enantiomers of the chiral substrates containing only alkyl substituents were also reduced relative to that of the wild type enzyme, but the reductions were smaller when compared to the reductions for the R_P-enantiomers containing a single phenyl substituent.

The steric constraints within the *small* subsite were successfully relaxed by the substitution of other residues found in this subsite with the dimensionally smaller amino acid, alanine. Mutation of Ile-106 or Ser-308 to alanine resulted in significant enhancements in the maximal rate of hydrolysis for the R_P-enantiomers containing a phenyl substituent. These results suggest that Ile-106 and Ser-308 play significant roles in dictating the substrate turnover of the wild type PTE for the R_P-enantiomers by sterically hindering the binding of a phenyl group to this region of the active site. The overall enhancements to the rates of hydrolysis of the R_P-enantiomers are greater for I106A than for S308A. Hence, the 20−90-fold stereoselectivity for the S_P-enantiomers with some of the chiral substrates was virtually eliminated upon mutation of Ile-106 to an alanine or substantially reduced by replacing Ser-308 with an alanine (Table 3). These results suggest that the *small* subsite of PTE largely dictates the chiral preference for the S_P-enantiomers by sterically hindering the approach or orientation of the R_P-enantiomers to the active site.

The crystal structure of PTE shows that Phe-132 primarily resides in the *leaving group* subsite. Mutation of Phe-132 to an alanine gave results that were somewhat unexpected. F132A displayed kinetic properties for the hydrolysis of organophosphate triesters that were very similar to those of I106A. With F132A, the rates of hydrolysis for the R_P-enantiomers of those substrates containing a single phenyl substituent were enhanced but no changes were observed for the corresponding S_P-enantiomers. The aromatic side chain of Phe-132 stacks with the indole group of Trp-131. Perhaps the replacement of the side chain of Phe-132 with a methyl group enables the indole ring of Trp-131, which resides between the *small* and *leaving group* subsites, to reorient more toward the *leaving group* subsite. Thus, the *small* subsite could be enlarged or reshaped and the steric restrictions for the phenyl substituent of the R_P-enantiomers reduced. Alternatively, mutation of Phe-132 to an alanine may cause other alternations within the *small* subsite in a way that the steric restrictions for the large substituents of the R_P-enantiomers are reduced. The crystal structure of the F132A mutant will be required to address this issue in more detail.

The side chains of His-254, His-257, Leu-271, and Met-317 are involved in the formation of the *large* subsite (*7*). Enlargement of this subsite through the construction of H254A, H257A, L271A, or M317A did not result in any significant increases in the catalytic rates for the S_P-enantiomers of the chiral substrates. Therefore, the large subsite must be capable of accommodating the large substituents without significant steric restrictions. For most of the substrates that were tested, the k_{cat} and k_{cat}/K_a values of these mutants were decreased relative to those of the wild type enzyme. Moreover, these four mutants did not cause an appreciable perturbation on the stereoselectivity for chiral substrates. These results suggest that some alterations may have occurred within the active site of PTE upon mutation of these four residues. It should be noted that His-254 is also a second-sphere ligand to the binuclear metal center through an ion pair with the primary metal ligand, Asp-301 (*15*).

The alteration of the three aromatic residues, Trp-131, Phe-306, and Tyr-308, was designed to probe the effects of mutations that originate primarily within the leaving group pocket of PTE. The mutation of W131 to an alanine resulted in reductions in the stereoselectivity for the S_P-enantiomers, which was a consequence of the reduced k_{cat}/K_a for the faster S_P-enantiomers combined with smaller changes in the values of k_{cat}/K_a for the slower R_P-enantiomers. These results indicate that the substitution of Trp-131 with an alanine may have caused a more global perturbation to the active site of PTE. Since the side chain of Trp-131 lies between the *small* and *leaving group* subsites, mutation of Trp-131 to an alanine may have decreased the steric restrictions for phenyl substituents for the R_P-enantiomers within the *small* subsite. The position of Phe-306 is unique within the crystal structure of PTE. This residue is actually positioned at the interface of the three binding pockets. Mutation of Phe-306 to an alanine resulted in significant reductions in the catalytic constant for most of the substrates that were tested. This result suggests that significant changes have occurred within the active site of PTE upon removal of the aromatic side chain of Phe-306. It can be inferred that replacement of the phenyl substituent with an alanine may have increased the size of the three binding pockets simultaneously, which may have resulted in a more global perturbation to the entire active site of PTE. Tyr-309 is located at the exit of the *leaving group* subsite with the side chain of this residue oriented away from the subsite. Mutation of this residue to an alanine had essentially no effect on the stereoselectivity for the S_P-enantiomers of the chiral substrates, but caused reductions in the catalytic constants for all of the substrates that were tested. This result indicates that mutation of Tyr-309 to an alanine may have disrupted the interactions of the aromatic side chain of Tyr-309 with other residues and perturbed the overall structure of the PTE.

The characterization of the 14 mutant enzymes with an organophosphate substrate library has identified the residues that are most important for the expression of the substrate specificity and stereoselectivity for PTE. The most significant residues are Gly-60, Ile-106, Phe-132, and Ser-308. With the native enzyme, it has been determined for organophosphates of the structural type presented in Figure 2 that the S_P-enantiomers are better substrates than the R_P-isomers. The X-ray structure of a bound inhibitor complex of PTE has outlined the binding subsites for the two nonleaving group substituents attached to the phosphorus core (*7*). The physically smaller substituent is preferred within the subsite anchored by Gly-60, while the larger substituent is preferred in the subsite containing Met-317. In this paper, we have unequivocally documented that the stereoselectivity and substrate specificity can be systematically manipulated by rather simple adjustments to the cavity size for the small subsite. This is a significant observation for the directed evolution and refinement of new catalytic activities within enzyme superfamilies.

When the physical size of the *small* subsite is diminished by the addition of a single methyl group, the stereoselectivity is significantly enhanced. For example, the stereoselectivity for the S_P- and R_P-isomers of methyl phenyl *p*-nitrophenyl phosphate (**IV**) increases from 90 to 13 000. This dramatic increase in the stereoselectivity has come about via the diminution in the rate of hydrolysis of the initially slower R_P-stereoisomer while the catalytic power for the hydrolysis of the initially faster S_P-stereoisomer has been maintained. Enhanced stereoselectivities of this type will enable PTE mutants to be utilized in the kinetic resolution of racemic organophosphate mixtures. This has practical significance since the synthesis of chiral organophosphate triesters by chemical means is difficult (*13*).

When the physical size of the *small* subsite is enlarged, the substrate specificity and stereoselectivity of PTE are relaxed. For example, the stereoselectivity for methyl phenyl *p*-nitrophenyl phosphate (**IV**) is reduced from 90 to 3 upon mutation of Ile-106 to an alanine residue. This relaxation phenomenon is due solely to the enhanced rate of turnover for the initially slower R_P-enantiomer while maintaining the catalytic power toward the hydrolysis of the initially faster S_P-isomer. Thus, for I106A the value of k_{cat}/K_a for (R_P)-methyl phenyl *p*-nitrophenyl phosphate (**IV**) is greater than 3 orders of magnitude higher than for G60A. However, the k_{cat}/K_a values for the S_P-isomer are within a factor of 3 of one another! This relaxation of the stereoselectivity through the enhancement of the initially slower isomer will be of significant benefit in the environmental detoxification of organophosphate nerve agents since many of these compounds are chiral at the phosphorus center. In the following paper, we elaborate on how the stereoselectivity can be reversed through a rational reconstruction of the active site structure.

ACKNOWLEDGMENT

We thank Dr. Craig Hill for his help with the construction of Figure 1.

REFERENCES

1. Donarski, W. J., Dumas, D. P., Heitmeyer, D. P., Lewis, V. E., and Raushel, F. M. (1989) *Biochemistry 28*, 4650−4655.
2. Dumas, D. P., Durst, H. D., Landis, W. G., Raushel, F. M., and Wild, J. R. (1990) *Arch. Biochem. Biophys. 277*, 155−159.
3. Caldwell, S. R., Newcomb, J. R., Schlecht, K. A., and Raushel, F. M. (1991) *Biochemistry 30*, 7438−7444.
4. Dumas, D. P., Caldwell, S. R., Wild, J. R., and Raushel, F. M. (1989) *J. Biol. Chem. 264*, 19659−19665.
5. Benning, M. M., Kuo, J. M., Raushel, F. M., and Holden, H. M. (1995) *Biochemistry 34*, 7973−7978.
6. Lewis, V. E., Donarski, W. J., Wild, J. R., and Raushel, F. M. (1988) *Biochemistry 27*, 1591−1597.
7. Vanhooke, J. L., Benning, M. M., Raushel, F. M., and Holden, H. M. (1996) *Biochemistry 35*, 6020−6025.
8. Hong, S. B., and Raushel, F. M. (1996) *Biochemistry 35*, 10904−10912.
9. Hong, S. B., and Raushel, F. M. (1999) *Biochemistry 38*, 1159−1165.
10. Boter, H. L., and Van Dijk, C. (1969) *Biochem. Pharmacol. 18*, 2403−2407.
11. Omburo, G. A., Kuo, J. M., Mullins, L. S., and Raushel, F. M. (1992) *J. Biol. Chem. 267*, 13278−13283.
12. Steurbaut, W., DeKimpe, N., Schreyen, L., and Dejonckheere, W. (1975) *Bull. Soc. Chim. Belg. 84*, 791−797.
13. Koizumi, T., Kobayashi, Y., Amitani, H., and Yoshii, E. (1977) *J. Org. Chem. 42*, 3459−3460.
14. Studier, F. W., and Moffatt, B. A. (1986) *J. Mol. Biol. 189*, 113−130.
15. Bullock, W. O., Fernandez, J. M., and Short, J. M. (1987) *BioTechniques 5*, 376−379.
16. Kuo, J. M., and Raushel, F. M. (1994) *Biochemistry 33*, 4265−4272.
17. Ho, S. N., Hunt, H. D., Horton, R. M., Pullen, J. K., and Pease, L. R. (1989) *Gene 77*, 51−59.
18. Watkins, L. M., Mahoney, H. J., McCulloch, J. K., and Raushel, F. M. (1997) *J. Biol. Chem. 272*, 25596−25601.

BI001548L